

# Sensorless three-phase induction motor direct torque control using sliding mode control strategy laboratory set-up for motor speed control teaching

Marcos Vinicius Lazarini and Ernesto Ruppert Filho  
Electrical and Computer Engineering School  
University of Campinas (UNICAMP) – Brazil  
lazarini@dsce.fee.unicamp.br, ruppert@fee.unicamp.br

**Abstract** - A three-phase induction motor direct torque control laboratory set-up for simulation and experimental activities is presented in this paper. It includes both PI controllers and sliding-mode controllers and uses a sensorless method to estimate rotor speed. The subject of this set-up is to present to the students a simulation tool based on Matlab SimPowerSystems toolbox with the possibility to check simulation results against a DSP based experimental system. The set-up provides to the electrical engineering students an excellent learning tool for non-linear control studies using as example the variable speed three-phase induction motor control.

*Index Terms* - induction motor, sensorless, sliding mode, torque control, simulation and experimental system

## INTRODUCTION

Among many control methods of induction machines, one of the most important today is the Direct Torque Control (DTC) method introduced by [1] and [2]. It can provide a very fast, accurate, reliable flux control and torque responses, and it is today one of the most important three-phase induction motor control method.

Sliding Mode Control (SMC) is presented today as a practical alternative to implement a discontinuous control and has some interesting advantages over the traditional control theory. As a discontinuous control, it has key advantages like the ability to be a very robust control, in many cases invariant to uncertainties and disturbances [5]; it has also properties of order reduction, decoupling design procedure and simple implementation in electric drives, since they have a natural “on-off” operating mode [8].

Sensorless drives are becoming more and more important as they can eliminate the speed sensor maintaining accurate response. Monitoring only the stator current and stator voltages, it is possible to estimate the necessary control variables. The observer type used here, a model-reference adaptative system (MRAS) [4], has presented good accuracy.

Simulation tools like Matlab/Simulink are becoming more and more important, following the computational power growth. Complex systems can be easily simulated, but they do not give the real experience to the students. Experimental systems are still complex and costly, being a real challenge to build them. However such activities are

very useful as a student learning environment and a non-linear control laboratory set-up is presented in this article.

The proposed set-up allows simulation activities of the complete system using developed Matlab SimPowerSystems models, where a concept of modular control algorithm permits that a block diagram can be easily replaced by other. Using the simulation block diagram students can program the DSP and use the DSP based experimental set-up to control a real machine. The DSP software was developed with modules concept in mind, providing a rich framework where students can use various implemented modules in experiments, closely related to simulations.

Using this constructed set-up the students can study, for example, the response of the various DTC controllers’ schemes and how they behave when the estimator has detuned parameters. The subject of the experimental set-up and the simulations developed is to show to the students many aspects of the non-linear systems using linear and non-linear controllers. This paper is going to show the theoretical foundations of the sensorless DTC of three-phase induction motor using sliding mode controllers and MRAS estimator.

## INDUCTION MOTOR CONTROL THEORY FUNDAMENTALS

Fundamentals of the induction motor control theory applied to the proposed students’ activities are summarized below.

### 1. Direct Torque Control

From the induction machine mathematical model above, the main equation of the direct torque control method [7] defines a relationship between the electromagnetic torque and the angle between the stator and rotor magnetic fluxes as shown in the relation

$$T_{em} = \frac{3}{2} \frac{P}{L_s L_r} \frac{L_m}{L_s L_r} |\Psi_s| |\Psi_r| \sin(\delta) \quad (1)$$

where  $T_{em}$  is the electromagnetic torque,  $P$  is the number of pole pairs,  $\Psi_s$  and  $\Psi_r$  are the stator and rotor windings linkage fluxes,  $L_s$  and  $L_r$  are the stator and rotor winding leakage inductances, and  $\delta$  is the angle between the stator and rotor winding magnetic flux vectors. Ignoring parameter variations, as long as the stator winding magnetic flux magnitude remains constant, the rotor winding magnetic flux magnitude will be constant too and, from (1), the electromagnetic torque is related only to the flux angle difference  $\delta$ .

The stator flux linkage vector depends directly on the stator voltages [9] and can be calculated as

$$\underline{\Psi}_s = \int (\underline{V}_s - r_s \underline{i}_s) dt \quad (2)$$

where  $V_s$  is the phase terminal voltage of the machine,  $r_s$  is the stator winding resistance, and  $i_s$  is the stator current. The underline denotes a 2-coordinate vector variable, the dq coordinate system. In most cases the ohmic voltage drop is small and can be neglected so the flux variations can be approximated considering  $r_s=0$ . Equation (2) shows that the flux variation is then due only to the applied stator voltage. In other words, to control the stator winding linkage flux vector, the inverter generates a stator voltage vector that moves the stator flux to a convenient position; this voltage vector is recalculated at each switching period.

The control algorithm calculates the magnitude and angle to move the stator flux winding linkage vector to a position producing torque according to (1). Flux vector magnitude is usually hold at rated value to generate the fastest possible response, but it is also possible to work with an underrated flux vector magnitude, in order to have lower acoustic noise and a better energy efficiency machine in specific situations at the cost of a slower response [1].

In the classical DTC control, the traditional two-level inverter can only produce 6 active and 2 inactive voltage vectors. This is an important constrain to the system and it is the cause of torque ripple in steady-state situations. Instead of the classical approach [1], using the space vector modulation strategy for a given fixed-time switching period, it is possible to generate a much wider range of average voltage vectors, producing a much more smooth and accurate response.

In order to find the correct magnitude and the new stator winding linkage flux vector position, the induction machine stator voltage equations [3] can be re-written. From [10], the dq components in the stationary reference frame are

$$\begin{aligned} V_{sd} &= r_s i_{sd} + \frac{d\Psi_s^*}{dt} \approx \frac{d\Psi_s^*}{dt} \\ V_{sq} &= r_s i_{sq} + \omega_s \Psi_s^* = \omega_s \Psi_s^* + \frac{r_s}{\Psi_s^*} T_{em} \end{aligned} \quad (3)$$

where superscripts \* means reference value and  $\omega_s$  is the synchronous angular speed of the stator flux vector. The above equations show, for a constant magnitude stator flux vector, that the d component of the stator voltage only affects the stator flux and can be used to control it directly. The q component of the stator voltage affects the torque variable, and if the term  $\omega_s \Psi_s^*$  is decoupled, it can be used to control the produced torque.

Figure 1 illustrates the control block diagram of the implemented DTC scheme. Of the two PI controllers shown, although recommended by some authors [11], one controller can be removed without significant penalty to the dynamics of the system. Because  $V_{sd}$  can be approximated to the variation of the stator flux according to (3), the stator winding linkage flux output error ( $|\Psi_s|^* - |\hat{\Psi}_s|$ ) already gives the proper variation and can drive  $V_{sd}$  directly.

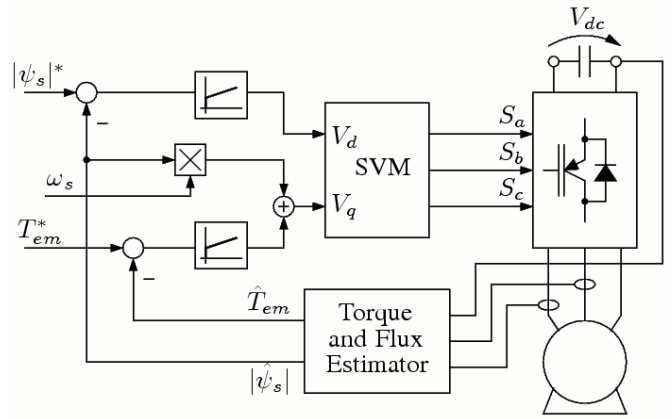


FIGURE 1  
DTC BLOCK DIAGRAM

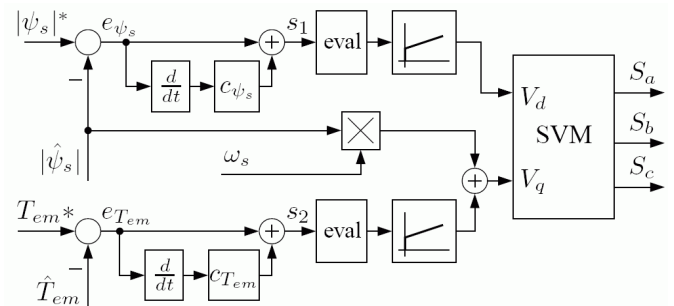


FIGURE 2  
DTC-SLIDING MODE CONTROL LAW

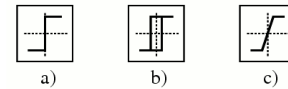


FIGURE 3

TYPICAL EVAL FUNCTIONS: A) SIGN, B) RELAY, C) LINEAR WITH SATURATION

## II. Sliding Mode Control

Sliding Mode Control is presented today as a feasible alternative to implement a robust control, taking advantage of the “on-off” inverter switches characteristics and its inherent discontinuous algorithm to control the electrical machine. However this causes a major disadvantage that is a variable switching frequency. In order to get a fixed switching frequency operation it is used the space vector modulation strategy that preserves the good characteristics of the sliding mode control. Implementation in discrete-time digital signal processor also demands changes to avoid unwanted chattering as explained below.

The sliding mode controller was designed to operate over the same variables used in the DTC method. The main goal of this approach is to obtain a sliding mode controller with all the qualities of DTC, which calculates the optimal stator voltage vector to maintain the stator winding linkage flux magnitude and angle within the desired ranges, and outputs this reference to the SVM inverter. The implemented block diagram is shown in Figure 2.

In this figure, the *eval* block usually is any function of the following family: sign, relay or linear with saturation as shown in Figure 3. Both the sign and the relay functions do not perform accurately in a discrete-time system, resulting in oscillations and undesired chattering. A linear function with

a proper gain provides much better results in reducing oscillations while still maintaining the properties of sliding mode [8].

The individual sliding surfaces are designed to behave in a similar way to the DTC control. First it is defined the error functions

$$\begin{aligned} e_{\Psi_s} &= |\Psi_x|^* - |\hat{\Psi}_s| \\ e_{T_{em}} &= T_{em}^* - \hat{T}_{em} \end{aligned} \quad (4)$$

where the hat symbol means estimated quantity and  $e$  is an error value to be minimized.

The sliding surface set  $S$  is defined from (4)

$$S = \begin{bmatrix} s_1 \\ s_2 \end{bmatrix} = \begin{bmatrix} e_{\Psi_s} + c_{\Psi_s} \frac{d}{dt}(e_{\Psi_s}) \\ e_{T_{em}} + c_{T_{em}} \frac{d}{dt}(e_{T_{em}}) \end{bmatrix} \quad (5)$$

where  $c_{\Psi_s}$  e  $c_{T_{em}}$  are constants to be defined according to the desired dynamic response.

The surfaces  $s_1$  and  $s_2$  were defined according to (3), using the same idea that the d stator voltage component is related with stator flux and q stator voltage component is related with electromagnetic torque.

The system control law is proposed in a similar way

$$\begin{aligned} V_{sd} &= \left( KP_{\Psi} + KI_{\Psi} \frac{1}{s} \right) eval(s_1) \\ V_{sq} &= \left( KP_T + KI_T \frac{1}{s} \right) eval(s_2) + \omega_s \hat{\Psi}_s \end{aligned} \quad (6)$$

where  $KP_{\Psi}$ ,  $KI_{\Psi}$ ,  $KP_T$  and  $KI_T$  are PI gains. The  $eval$  function is implemented as a linear gain with saturation

$$eval(x) = \begin{cases} xk_{ev} & \text{if lower limit} < x < \text{upper limit} \\ \text{upper limit} & \text{if } x > \text{upper limit} \\ \text{lower limit} & \text{if } x < \text{lower limit} \end{cases} \quad (7)$$

where  $k_{ev}$  is a constant related to the system dynamics.

The system's state can start outside the sliding surface but it will be driven in the direction of the sliding surface as control effort will be produced according to (6) to reduce the errors (4) and to reach  $S=0$ . This phase of the process is named the *reaching phase*.

When the system state reaches the  $S=0$  surface and enters in the *sliding phase* or sliding mode, the control law (6) restricts the state to the slide surface  $S$  and the system actions is governed by the dynamics imposed by  $S=0$  only. The system state is not allowed to leave the surface, generating a quick and large control effort to keep the system state very close to the sliding surface. This intense reaction, besides producing a very fast response, can also generating undesired ripple, as a side-effect of limit cycle in the state space plane. Using the linear function from Figure 3 and with proper gains, the system response is fast and stable.

The equivalent control is a fundamental theory in variable structure systems that simplify the discontinuous system analysis, replacing discontinuous equations with continuous equivalents, where its trajectory is the sliding surface itself. Therefore it is possible to calculate traditional coefficients, like damping factor and natural frequency for a

step response for example. A more detailed view of the background theory and sliding surface design is shown in [8].

### III. Estimator Subsystem

The adopted estimation structure is a model-reference adaptive system *MRAS* [4], and it consists of three stage system: two independent estimators and an adaptive mechanism to correct the estimations, producing the final result. An improved model, discussed in [6], was the basic scheme. The adopted structure is presented in Figure 4.

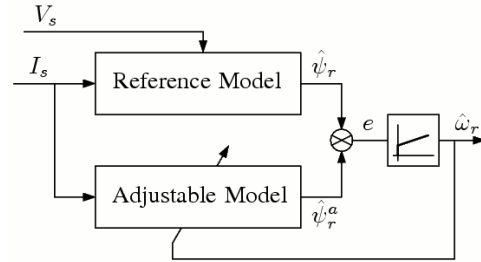


FIGURE 4  
MRAS BLOCK DIAGRAM

#### A. Reference Model

The reference model discussed here is adaptive itself. The rotor winding linkage flux is calculated from a closed loop system. This method, analyzed in details in [6], uses two distinct reference frames to get an improved estimation. The stationary and rotor flux reference frames were used.

Using the rotor flux reference frame, the rotor flux equations are simpler to be described: the d axis is aligned with the rotor flux and receives all the flux contribution, with the q, perpendicular to the rotor flux, receiving no contribution. Thus, the rotor flux in rotor flux reference frame can be written as

$$\underline{\Psi}_r^r = \begin{bmatrix} \Psi_{rd}^r \\ \Psi_{rq}^r \end{bmatrix} = \begin{bmatrix} L_m / (1 + sT_r) \cdot i_{sd}^r \\ 0 \end{bmatrix} \quad (8)$$

where  $L_m$  is the machine magnetizing self-inductance,  $T_r$  is the rotor time-constant and superscript r denotes variable in the rotor flux reference frame. It is interesting to note that this model uses only stator currents and some machine parameters.

Performing a coordinate system conversion of (8) to the stationary reference frame, the stator flux can be calculated from the rotor flux and stator current as

$$\underline{\Psi}_s^i = \frac{L_m}{L_{lr}} \underline{\Psi}_r^r + \frac{L_{ls}L_{lr} - L_m^2}{L_{lr}} \underline{i}_s \quad (9)$$

The superscript i denotes the stator flux calculated from the stator currents.

The reference model also calculates the stator flux with another method, through a feedback system where the stator flux estimation  $\Psi_s$  is the feedback variable. A PI compensator - represented by  $(KP_{\Psi}^e + KI_{\Psi}^e / s)$  - dictates the error contribution between the flux estimations (9) and (10)

$$\underline{\hat{\Psi}}_s = \frac{1}{s} \left( \underline{V}_s - r_s \underline{i}_s - \left( KP_{\Psi}^e + \frac{KI_{\Psi}^e}{s} (\underline{\hat{\Psi}}_s - \underline{\hat{\Psi}}_s^i) \right) \right) \quad (10)$$

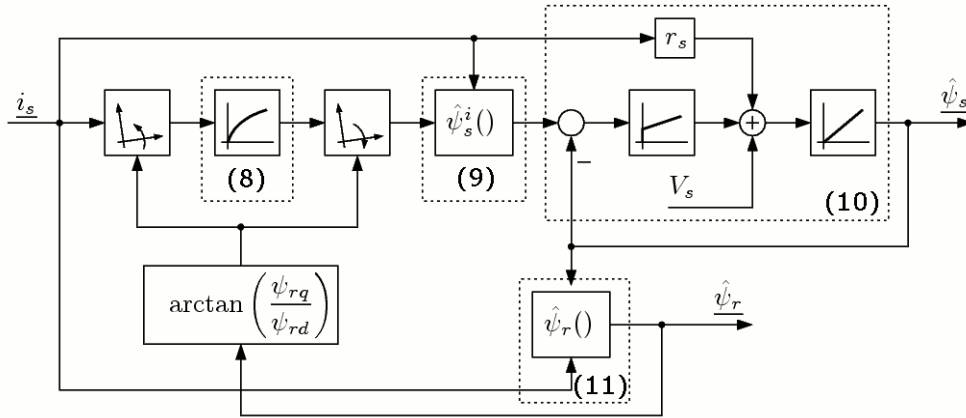


FIGURE 5  
MRAS REFERENCE MODEL

The superscript  $e$  is used to avoid confusion with others PI compensators gains. This model uses now stator currents and voltages. This PI compensator is used to correct pure integrator errors and small stator resistance variation through the voltage model estimation.

The reference model final rotor flux estimation value  $\Psi_r$  is calculated from stator voltages and currents by

$$\frac{\hat{\Psi}_r}{L_m} = \frac{L_{lr}}{L_m} \frac{\hat{\Psi}_s}{L_m} - \frac{L_{ls}L_{lr} - L_m^2}{L_m} \dot{i}_s. \quad (11)$$

### B. Adjustable Model

The adjustable or adaptative model equation is simpler and is obtained from the current model of the machine equations in stationary reference frame [4] using stator currents and rotor angular velocity

$$\frac{\hat{\Psi}_r^a}{L_m} = \begin{bmatrix} (-1/T_r) & -\hat{\omega}_r \\ \hat{\omega}_r & (-1/T_r) \end{bmatrix} \frac{\hat{\Psi}_r^a}{L_m} + \frac{L_m}{T_r} \dot{i}_s. \quad (12)$$

The superscript  $a$  denotes the stator flux calculated from the adaptative model.

### C. Rotor speed estimation

With the rotor flux estimation from two methods - the voltage model  $\Psi_r$  (reference model) and the current model  $\Psi_r^a$  (adaptative model) - the rotor speed estimation  $\hat{\omega}_r$  can be calculated with a PI adaptation mechanism by

$$\hat{\omega}_r = \left( KP_\omega + \frac{KI_\omega}{s} \right) \cdot e \quad (13)$$

where

$$e = \hat{\Psi}_{rd}^a \hat{\Psi}_{rq} - \hat{\Psi}_{rq}^a \hat{\Psi}_{rd} \quad (14)$$

is the cross-error between the adjustable and reference models.

## SIMULATION ACTIVITIES

Simulation tools play a fundamental role in today's engineering educational projects. Using a mathematical model of a given plant, the simulation provides valuable information about the dynamic behavior of the plant, avoiding the high costs of equipment and risk of accidents. The three-phase electric machine model is complex and non-

linear, and some small impact simplifications and linearizations are made. Thus, after gaining some experience with the simulation, the students should have an experience with the real system, to test the controllers they have designed and simulated, during the experimental activities using the proposed set-up.

The machine parameters used in the simulation are the same got from the real machine and the system operates in closed-loop with speed feedback from tacogenerator or from the MRAS estimator.

Typical tests situations of a sensorless induction motor control include the load torque step change, reference speed step reversal, reference speed ramp reversal and low speed operation tests.

The proposed simulated scenarios shown in this paper covers the following situations: a step change in the speed reference (from 0.5 pu to -0.5 pu) and a step change in torque (from 0 to 0.5 pu).

The results of step change in the speed reference are presented in Figure 6, where the real speed and estimated speed are shown. Although with some oscillations, the estimation tracked the real speed very close and it was able to follow the rotor speed within 5% accuracy most of the time.

The stator flux is also estimated and is shown in Figure 7. During the start up phase, the stator flux grows from zero to the rated value. The flux magnitude is held constant from this moment on, and this can be verified that the stator flux locus in a xy plane is a circle.

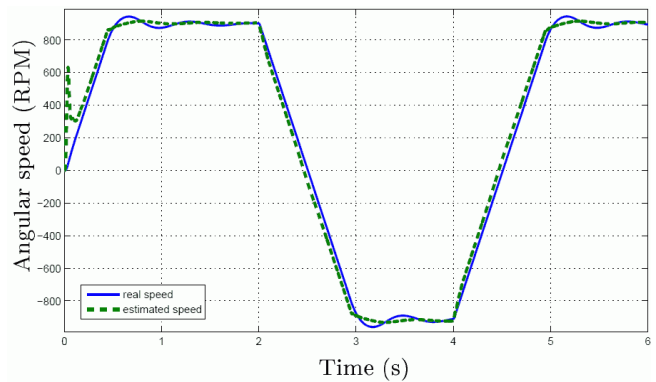


FIGURE 6  
SYSTEM RESPONSE TO THE REFERENCE SPEED STEP CHANGE  $\pm 0.5$  PU

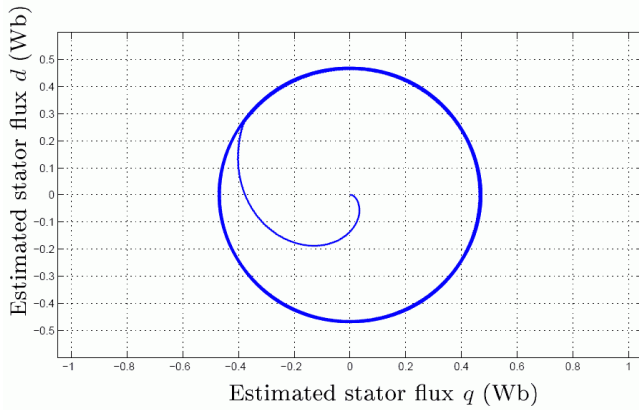


FIGURE 7  
STATOR FLUX DURING THE SPEED STEP CHANGE TEST

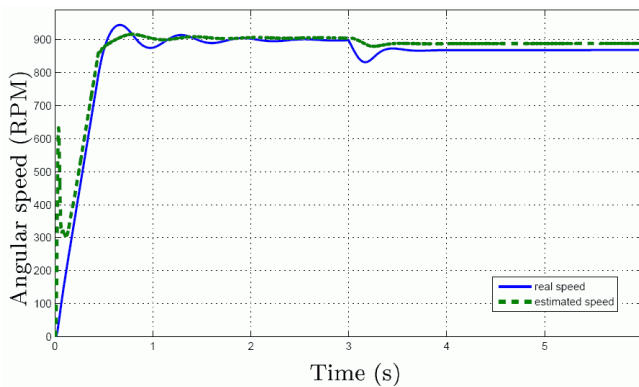


FIGURE 8  
SYSTEM RESPONSE TO THE LOAD TORQUE STEP CHANGE 0.5 PU

The step change in the torque, from 0 to 0.5 pu at 50% rated speed is shown in Figure 8. Operating at no load, the speed estimation almost matches the real speed; with 0.5 pu load, the system settle to a new steady state, where the difference between the real and the estimated speed is less than 2%.

The learning activities can also include changes in the controllers' parameters, detuned estimator gains, changes in the motor parameters, autoclosing and changes in the controller types to see their effects on the system response.

### EXPERIMENTAL ACTIVITIES

The experimental activities are realized using the set-up proposed in this article. It includes electronic circuits and electro-mechanical devices. Figures 9 and 10 display the built experimental setup during the development phase.

The experimental set-up consists of a DSP (Texas Instruments TMS320F2812) connected to an induction motor, driven by a 6 kW Semikron three-phase inverter (SKS 27F B6U + B6CI 10V06).

The induction motor has a moving frame proper for the electromagnetic torque measurement. Load torque can be measured directly in the shaft using another load cell. The load torque that is the torque available at the shaft can also be calculated as the electromagnetic torque minus the losses caused by ventilation and friction. The load is a DC machine operating as a DC generator, delivering the produced power to a load rheostat. This configuration allows the calculation

of the load torque using the voltages and currents produced by the DC generator.



FIGURE 9  
EXPERIMENTAL SET-UP SHOWING THE ELECTROMECHANICAL SET (INDUCTION MOTOR AND ITS LOAD) AND THE DRIVING SET

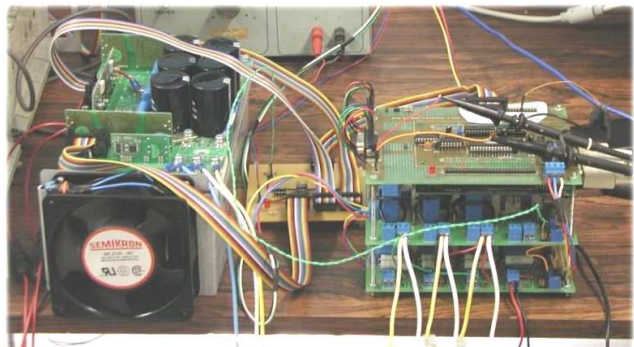


FIGURE 10  
INVERTER (LEFT) AND THE CONTROL CIRCUITS TOWER (DSP AND CONDITIONING CIRCUITS)

The used DSP is a high-performance 32 bits RISC Texas Instruments, model TMS320F2812, and runs at 150 MHz. It is able to do complex calculations in real-time, like sophisticated speed estimation methods and digital motor control, operating at a high switching frequency of 10 kHz. The DSP has many built-in peripherals, as a 16 channel AD converter and 2 independent PWM modules, providing a lot of resources to implement digital motor control without many external devices.

Texas Instruments provides a very complete set of digital motor control foundation libraries, supporting an easy and stable environment for the implementation of the algorithms in a fast pace, an appropriate condition to an educational experiment. Additional routines to control specific sub-systems as, e.g., the conditioning signals circuits, the AD converter and the inverter, were developed and are provided. This way the student can focus on the control algorithm.

A three-phase inverter produced by Semikron is driven by the DSP. It is a 6 kW inverter, using modules SKS 27F B6U and B6CI 10V06. The DSP has complete access to the inverters IGBTs, allowing the engineer to choose between

pre-defined hardware imposed or DSP software controlled dead-time. This permits fine control over the quality of the generate PWM signals, supporting future studies related to unwanted harmonics and EMI effects.

Conditioning signal boards are necessary to acquire the motor state variables from a high level of voltage and current to an appropriate voltage level to be sampled and converted by the internal AD converter. Software routines are provided to remove the residual mean value of AC signals.

An oversampling technique is used to sample the voltages and currents. Thanks to the powerful DSP the sampling frequency can be defined as eight times the switching frequency (i.e. 80 kHz) and a moving average filter with a uniform weight of 1/8 is used to smooth the sampled signal. This method has many advantages over traditional sampling and is also available to the students.

Figure 11 shows the speed reversal test, varying between +30 Hz and -30 Hz each 2s. In this test, the estimator gave good results, as both signals were almost superimposed; the steady state error is below 2%. The Figure 11 also shows that the braking is faster than the acceleration, because the friction force wasn't considered in the equations of the motor dynamic mathematical model, but it wasn't negligible in this machine.

In a much similar situation to the presented in Figure 8, the experimental set-up has produced the output shown in Figure 12. Although the estimator was not able to track the real speed closely, the oscillations were minimal.

## CONCLUSION

The main goal of this paper is to propose a laboratory set-up for simulation and experimental activities in a three-phase induction motor direct torque control experiment, offering a great learning experience about non-linear control to the students. Different controllers (PI and sliding-mode controllers) and a sensorless method to estimate rotor speed can also be used and their responses can be analyzed. Results are very clear, illustrative and proper to prepare several types of learning activities according to the instructor imagination.

The proposed set-up and activities allow electrical engineering students (undergraduate and graduate) to experience the difficulties and particularities of non-linear systems and non-linear controllers. Using as example the variable speed three-phase induction motor control, there are plenty of good situations to be exploited by the faculties and the assistant teachers enrolled with the teaching of control and electrical machines.

## ACKNOWLEDGMENT

The authors are grateful to FAPESP – the State of São Paulo Research Foundation – and to CNPq – Brazilian National Research Council – for the financial support and to Texas Instruments for the DSP donation.

## REFERENCES

- [1] I. Takahashi and T. Noguchi, "A new quick response and high efficiency control strategy of an induction motor," *Industry Applications, IEEE Transactions on*, vol. 22, pp. 820–827, 1986.
- [2] M. Depenbrock, "Direct self-control (DSC) of inverter-fed induction machine," *Power Electronics, IEEE Transactions on*, vol. 3, no. 4, pp. 420–429, 1988.
- [3] Y. Xue, X. Xu, T. Habetler, and D. Divan, "A low cost stator flux oriented voltage source variable speed drive," in *Industry Applications Society Annual Meeting, 1990., Conference Record of the 1990 IEEE*, 1990, pp. 410–415 vol.1.
- [4] C. Schauder, "Adaptive speed identification for vector control of induction motors without rotational transducers," *Industry Applications, IEEE Transactions on*, vol. 28, no. 5, pp. 1054–1061, 1992.
- [5] J. Hung, W. Gao, and J. Hung, "Variable structure control: a survey," *Industrial Electronics, IEEE Transactions on*, vol. 40, no. 1, pp. 2–22, 1993.
- [6] P. Jansen, R. Lorenz, and D. Novotny, "Observer-based direct field orientation: analysis and comparison of alternative methods," *Industry Applications, IEEE Transactions on*, vol. 30, no. 4, pp. 945–953, 1994.
- [7] P. Vas, *Sensorless Vector and Direct Torque Control*. Oxford University Press, 1998, ISBN: 0198564651.
- [8] V. Utkin, J. Guldner, and J. Shi, *Sliding Mode Control in Electromechanical Systems*. CRC Press, 1999, ISBN: 0748401164.
- [9] M. P. Kazmierkowski, *Control in Power Electronics: Selected Problems (Academic Press Series in Engineering)*. Academic Press, 2002.
- [10] G. Buja and M. Kazmierkowski, "Direct torque control of PWM inverter-fed AC motors - a survey," *Industrial Electronics, IEEE Transactions on*, vol. 51, no. 4, pp. 744–757, 2004.
- [11] C. Lascu, I. Boldea, and F. Blaabjerg, "Direct torque control of sensorless induction motor drives: a sliding-mode approach," *Industry Applications, IEEE Transactions on*, vol. 40, no. 2, pp. 582–590, 2004.

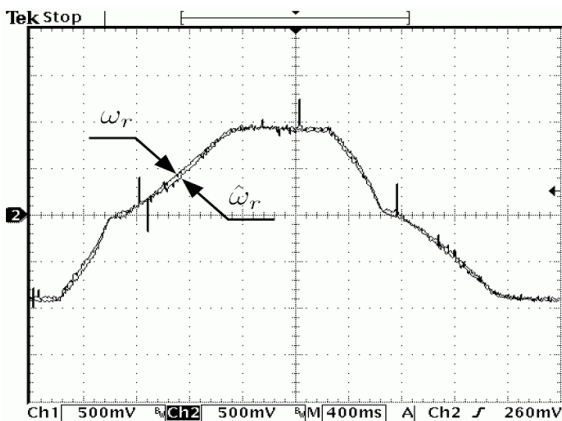


FIGURE 11

REAL AND ESTIMATED ROTOR SPEED IN STEP CHANGE,  $\pm 30$  Hz (10 Hz/DIV)

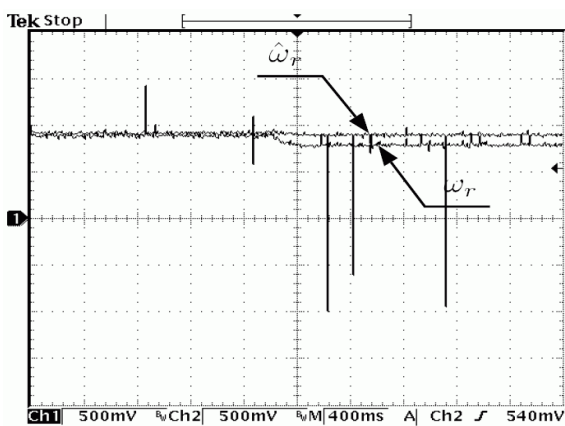


FIGURE 12

SPEED RESPONSE TO A 0.5 PU TORQUE STEP CHANGE AT 30 Hz